Hindawi
Advances in Meteorology
Volume 2018, Article ID 6941501, 13 pages
https://doi.org/10.1155/2018/6941501

Research Article

Investigation of Vorticity during Prevalent Winter Precipitation in Iran

Iman Rousta,[1,2] **Farshad Javadizadeh**,[3] **Fatemeh Dargahian**,[4] **Haraldur Ólafsson**,[5] **Amin Shiri-Karimvandi**,[6] **Sayed Hossein Vahedinejad**,[7] **Mehdi Doostkamian**,[6] **Edgar Ricardo Monroy Vargas**,[8] **and Anayat Asadolahi**[6]

[1]*Department of Geography, Yazd University, Yazd 8915818411, Iran*
[2]*Senior Researcher, Institute for Atmospheric Sciences, University of Iceland and Icelandic Meteororological Office (IMO), Bustadavegur 7, IS-108 Reykjavik, Iceland*
[3]*Department of Environment, Collage of Natural Resource, Bandar Abbas Branch, Islamic Azad University, Bandar Abbas, Iran*
[4]*Desert Research Division, Research Institute of Forests and Rangelands, Agricultural Research Education and Extension Organization (AREEO), Tehran, Iran*
[5]*Department of Physics, University of Iceland, Institute for Atmospheric Sciences and Icelandic Meteororological Office (IMO), Bustadavegur 7, IS-108 ReykjaviK, Iceland*
[6]*Department of Geography, University of Zanjan, Zanjan 3879145371, Iran*
[7]*Department of Geography, University of Kharazmi, Tehran 1491115719, Iran*
[8]*Department of Civil Engineering, Universidad Catolica de Colombia, Bogotá, Colombia*

Correspondence should be addressed to Iman Rousta; irousta@yazd.ac.ir and Farshad Javadizadeh; javadizadeh2020@yahoo.com

Received 20 February 2018; Revised 19 March 2018; Accepted 5 April 2018; Published 30 September 2018

Academic Editor: Andrew D. Jensen

In this study, precipitation data for 483 synoptic stations, and the U&V component of wind and HGT data for 4 atmospheric levels were respectively obtained from IRIMO and NCEP/NCAR databases (1961–2013). The precipitation threshold of 1 mm and a minimum prevalence of 50% were the criteria based on which the prevalent precipitation of Iran was identified. Then, vorticity of days corresponding to prevalent winter precipitation was calculated and, by performing cluster analysis, the representative days of vorticity were specified. The results showed that prevalent winter precipitation vorticity in Iran is related to the vorticity patterns of low pressure of Mediterranean-low pressure of Persian Gulf dual-core, low pressure closed of central Iran-high pressure of East Europe, Ural low pressure-Middle East High pressure, Saudi Arabia low pressure-Europe high pressure, and high-pressure belt of Siberia-low pressure of central Iran. At the same time, the most intense vorticity occurred when the climate of Iran was influenced by a massive belt pattern of Siberian high pressure-low pressure of central Iran. However, at the time of prevalent winter precipitation in Iran, an intense vorticity is drawn with the direction of Northeast and Northwest from the center of Iraq to the south of Iran.

1. Introduction

Changes in extreme weather and climate events have significant impacts and are among the most serious challenges to society in coping with a changing climate [1–9]. The most important factor in the formation and guidance of atmospheric systems is vorticity process [10–12]. In the middle latitudes, at the synoptic scale, the important dynamic properties are those which are related to rotating particles in the air [13]. Dessouky and Jenkinson [14]and Jenkinson and Collison [15]are two examples of studies in different parts of the world focusing on the role of vorticity conditions and amount at different atmosphere levels in precipitation. Based on the general format of weather types identified by Lamb, Dessouky and Jenkinson investigated vorticity and the direction of flows in pressure systems producing severe storms in the UK, and systems producing drought and wet years in Egypt [14]. Jenkinson's method has been tested by many researchers in different areas

of the world. They showed that using this method can make it possible to identify weather types and quantitatively calculate their intensity and weakness. Since the convergence leads to upside movements, some studies have investigated vorticity advection, divergence, and vertical motions combined with high levels of atmosphere jet stream as an evidence for the development of surface low pressure [16–19]. In another study, Nakamura showed that high levels of jet stream simultaneously occur with divergence and relative positive vorticity advection [20]. Different case studies show that the presence and intensity of relative positive vorticity advection with the vertical arrangement of the wind caused by the jet stream changes provide favorable conditions for increasing vertical movements and uplink, and creating low surface pressure [21–23]. Vincent studied the development of cyclones in the South Pacific convergence zone using vorticity [24]. In another study, Wang examined the relative vorticity of ocean winds and its impact on the development of tropical cyclones in the South China Sea. He concluded that the winter tropical cyclone genesis in the South China Sea happens due to vertical shear of the horizontal winds and low-level atmospheric vorticity [25]. In other studies around the world, Alpert et al. investigated the horizontal distribution and the vertical profile of the relative vorticity over the Mediterranean region over a period of 5 years [26]. Bartzokas and Metaxas estimated the seasonal values of the geostrophic relative vorticity at four grid points in the Mediterranean by using pressure data for the period 1873–1988 [27]. Ruiz and Vargas studied the 500 hPa vorticity distribution over Argentina and its association with large-scale precipitation on a climatological basis [28]. Xoplaki et al. studied the wet season Mediterranean precipitation variability, and showed that since the mid-nineteenth century, precipitation steadily increased with a maximum in the 1960s and decreased since then [29]. There are a few climatological studies of vorticity in Iran. Golmohammadian and Pishvaie is one of the research projects concentrating on the relationship between vorticity and other synoptic indicators in Iran. This study used the model of area circulation to create monthly vorticity indicators in south of Iran for eight points on two surfaces of land and 500 hPa. The results showed that there is a trough in the East Mediterranean during all months of the year, and vorticity indicators with temperature are better than precipitation in analyzing the climatic responses to the selected station of Shiraz [30]. Alijani and Zahehi analyzed Azerbaijan precipitation to statistically and synoptically determine the types of air masses affecting this area. For this purpose, the daily precipitation data of the Tabriz station for the period of 1961–1995 and also pressure data at 12 am at ground level and 500 hPa were used. Consequently, 11 types of air masses in the precipitation of Azerbaijan were identified, with only 3 of them being high pressure [31]. In another study, Meshkati and Moradi examined the pressure trough of the Red Sea from the dynamic viewpoint, revealing that if the advection of relative positive vorticity takes place in the east of the Mediterranean or north of the Red Sea, the pressure trough of the Red Sea moves to the east of the Mediterranean Sea and influences the west and northwest of Iran. On the other hand, if the advection of relative positive vorticity occurs in the northeast of the Red Sea, small low-pressure cells are separated from the trough of pressure on the Red Sea and move towards the northeast and affect the west, southwest, and south of Iran [32]. In contrast, Mofidi et al. investigating fall precipitation in the northern coast of Iran, showed that a high-pressure center on the west of the Caspian Sea and negative vorticity on the sea in lower levels of the atmosphere combined with strong currents and prevailing in the north-south direction are the main factors causing heavy and extreme fall precipitation in all the synoptic patterns of the Caspian [33].

The objective of this study is to investigate the vorticity over the prevalent winter precipitation in Iran, for a period of 53 years, along with its seasonal variations. This study, thus, seeks to understand from a climatological point of view the dynamic background of the troposphere over the regions that have an effect on the occurrence of prevalent winter precipitation in the study area. Furthermore, it is intended to gain a better insight into the dynamic mechanisms responsible for this kind of precipitation in Iran. Since prevalent and extreme precipitation is a dangerous phenomenon that will have environmental damages, especially in areas with small amounts of annual precipitation (e.g. Iran), it is critical to study the dynamic features that can help to better identify such precipitation. According to studies conducted by researchers inside and outside Iran, it is crucial to review the vorticity status of the atmosphere in prevalent winter precipitation in Iran. This can lead to an understanding of the relationship between atmospheric rotations and the surface environment of land in order to recognize different states of vorticity and their impact on convergence and divergence at different levels of the atmosphere, leading to the identification of prevalent precipitation in Iran. Therefore, in this study, we have tried to study the vorticity patterns leading to prevalent winter precipitation in Iran.

2. Materials and Methods

This study sought to examine the vorticity status of the atmosphere during prevalent winter precipitation in Iran. To this end, winter precipitation data of 483 stations were gathered from the Meteorological Organization of Iran (IRIMO). The spatial distribution of stations is shown in Figure 1. After sorting, a database with the size of 7187×4383 was formed for a period of 53 years. Then, prevalent winter precipitation data were extracted from precipitation data with a minimum amount of a millimeter.

After the formation of database, three criteria were taken into account to determine the days with prevalent precipitation:

(1) A minimum precipitation of one mm during the specific day

(2) A precipitation lasting for at least two consecutive days

(3) A precipitation covering at least 50% of the area (spatial continuity condition)

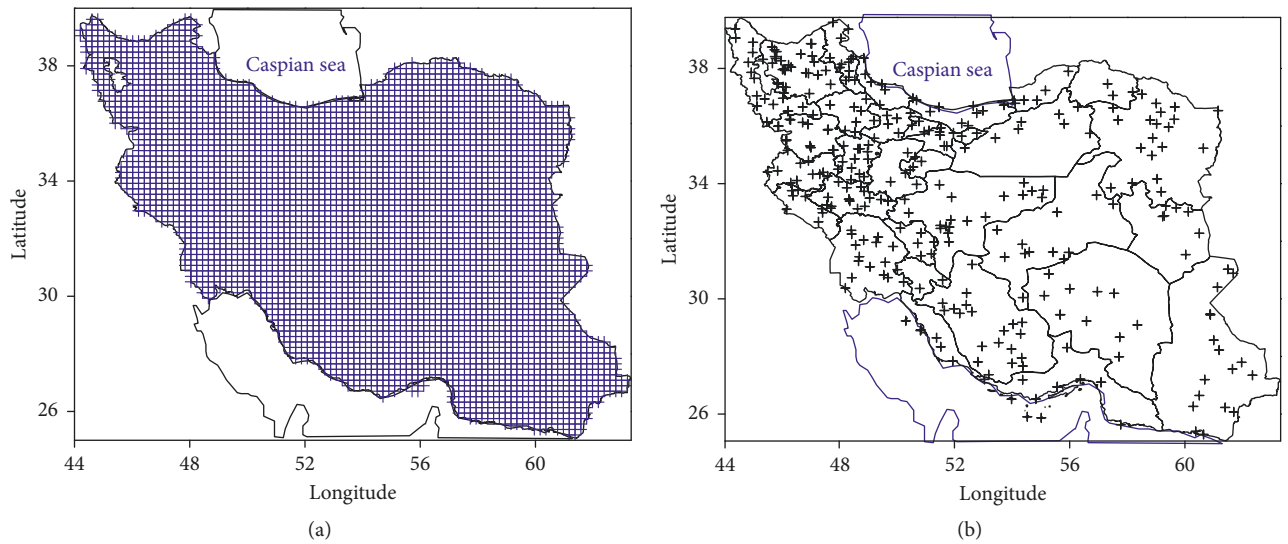

Figure 1: Regular grid of the precipitation database (a) and spatial distribution of studied stations (b).

By setting the conditions, just prevalent precipitation were selected for each of the cells studied and the relative concept of prevalent precipitation was observed for different regions of the country. The second criterion was having the precipitation for at least 2 consecutive days. Using this criterion, we were able to make a distinction between precipitation with a systematic (synoptic) origin and local precipitation that occurred due to convection or topography. After extracting the prevalent winter precipitation, pressure and U&V wind component data corresponding to the prevalent rainy days were extracted from NCEP/NCAR database with a spatial resolution of 2.5×2.5 degree [34]. Finally, using the programming in GrADS software [35], vorticities of 1000, 850, 700, and 500 hPa for the days with prevalent precipitation were calculated

The vorticity is a vector quantity defined as the curl (cross-product) of the velocity vector. The relative vorticity is given as follows [36]:

$$\vec{U} = \nabla \times \vec{V} = \left(\frac{\partial w}{\partial y} - \frac{\partial v}{\partial z}\right)\hat{i} + \left(\frac{\partial u}{\partial z} - \frac{\partial w}{\partial x}\right)\hat{j} + \left(\frac{\partial v}{\partial x} - \frac{\partial u}{\partial y}\right)\hat{k}. \tag{1}$$

In Cartesian coordinates, a large fraction of the rotating fluid systems with which we are interested exhibit rotation in the horizontal plane (i.e., midlatitude cyclones, hurricanes, and tornadoes). Consequently, dynamic meteorology is most often, though not exclusively, interested in the vertical component of the relative vorticity. It is generally expressed as follows [36]:

$$\zeta = \hat{k}.\vec{u} = \hat{k}.\nabla * \vec{V} = \frac{\partial v}{\partial x} - \frac{\partial u}{\partial y}. \tag{2}$$

In the northern hemisphere, a positive vorticity indicates a cyclonic motion and a negative vorticity demonstrates an anticyclonic motion. Anticlockwise and clockwise movements are respectively called cyclonic and anticyclonic movement [32,37–40].

Subsequently, cluster analysis of 1000 hPa vorticity was used in order to identify vorticity patterns of prevalent winter precipitation in Iran. In the next step, the result of this cluster analysis was obtained with the aim of classifying the atmospheric vorticity data and detecting representative days. Cluster analysis is a method where the variables are classified based on the characteristics desired in certain groups. The aim of cluster analysis is to find out the real groups of people and reduce the volume of data. In other words, the aim is to identify a smaller number of groups so that similar data are grouped together in a way that within-group variation is minimized and between-group variation is maximized. In this method, data are grouped based on the distance or similarity between them. There are several ways to measure the distance between the data. One of the most popular methods is the Euclidean distance [7]. Lund correlation method was used in order to choose the representative days of groups derived from classifying data on atmospheric vorticity. Thus, a representative day of a particular group is the one with the highest similarity to the maximum number of days in the group. The correlation coefficient indicates the degree of similarity of patterns of two maps. But a certain correlation coefficient threshold must be determined. The correlation coefficient value in such cases typically varied between 0.5 and 0.7 [41]. In the current study, the cut-off point for identifying the representative days was a correlation coefficient of 0.5. Thus, the day with the highest number of correlation coefficient values greater than 0.5 with other days of the same group was regarded as the representative day.

3. Results and Discussion

Five patterns were identified as a result of the implementation of cluster analysis on 1000 hPa data with prevalent winter precipitation. The results are displayed in Figure 2 and Table 1.

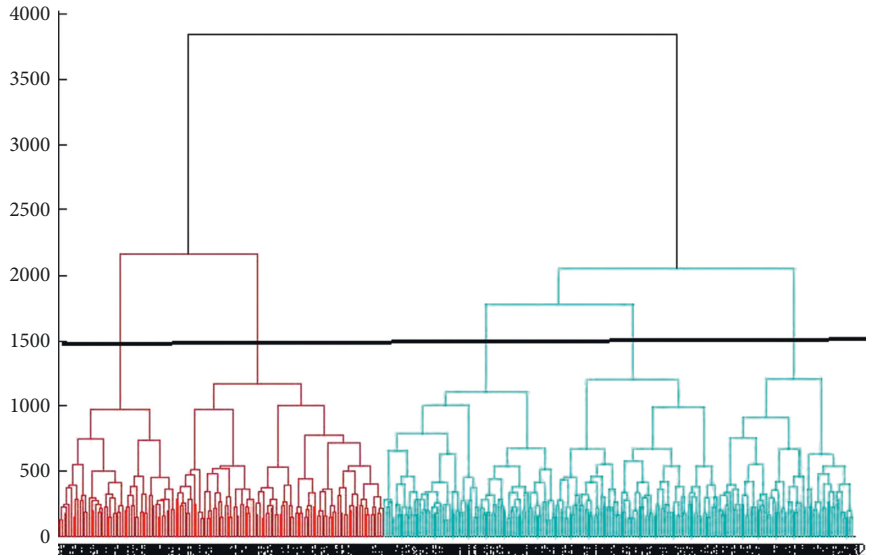

Figure 2: Dendrogram of cluster analysis on the Earth's surface pressure data.

Table 1: Some of the characteristics of identified patterns of prevalent winter precipitation in Iran.

1000 hPa vorticity patterns	Prevalence percentage	Overall precipitation	Frequency
Mediterranean low pressure-low-pressure dual-core Persian Gulf	50.132	3603	77
Iran closed low pressure-high pressure of east Europe	81.035	5824	73
Low pressure of Ural-high pressure of the Middle East	56.992	4096	60
European high pressure-low pressure of Saudi Arabia	58.314	4191	52
High-pressure belt of Siberia-low pressure of central Iran	55.322	3976	93

It is observed that the longest winter precipitation pattern in Iran (with a frequency of 93 days) occurred when the Siberian high-pressure belt-central Iran low pressure prevailed over Iran. On the other hand, the largest amount of overall precipitation in Iran happened when the low pressure of central Iran-high pressure of East Europe dominated the country (Table 1). However, at the time of the precipitation pattern of low pressure of the Mediterranean-low pressure of the Persian Gulf dual-core, the overall amount of precipitation reached 3603 mm.

In what follows, we provide a detailed description of the experimental results, present our interpretation, and draw a number of experimental conclusions.

3.1. The First Pattern: Low Pressure of Persian Gulf Dual-Core-Low Pressure of East Mediterranean. As illustrated in Figure 3(a), the pressure and vorticity is 1000 hPa on Iran, and because of the exposure to dual-core low pressure in the Persian Gulf, the wind velocity is lower in the pole part; finally, in the eastern part of the low-pressure system, mass and density increase, and by increasing pressure, convergence will occur. While in its western part, due to the reduction of input mass from the north and increasing output mass from the southern part in the middle band, the mass and density are reduced and thus divergence will occur. However, the divergence of airflow in the low-pressure west of the Persian Gulf caused decreased airflow on the surface and vorticity advection of $-2.5 \times 10^{-5}_{S^{-1}}$ (m/s) on Iran's southern half. However, Lashkari showed that in a low-pressure flow, depending on the density of air and the input flow of air to its east, convergence occurs, and in its western part, divergence occurs due to the high speed of airflow [42–45]. Such a situation is clearly shown in Figure 3(a). On the other hand, the exposure of the west and northwest of the country to the East Mediterranean low pressure (wave front) caused a vertical rise and the convergence of airflow from a lower width at 1000 hPa (Figure 3(a)). So, the position of the low-pressure systems is critical because the systems usually have the strongest winds and the greatest waves [46]. With this interpretation, at the level of 850 hPa (Figure 3(b)) on Iran, positive vorticity advection of $-2.5 \times 10^{-5}_{S^{-1}}$ can be seen, which represents the planetary flows and vertical movements in the balance. As observed, vorticity minimum area on the north of the Black Sea can be detected coinciding with the full-height center of 1540 geopotential m that flows downward in a clockwise manner onto the northwest regions of the country.

Considering the amount of vorticity at 850 hPa, positive vorticity advection causes the flow of convergence on the lower level and intensification of flow of divergence in the upper level of the atmosphere [47]. On the other hand, at the levels of 700 and 500 hPa (Figures 3(c) and 3(d)), in accordance with the model 850 hPa, low-height center of 2960

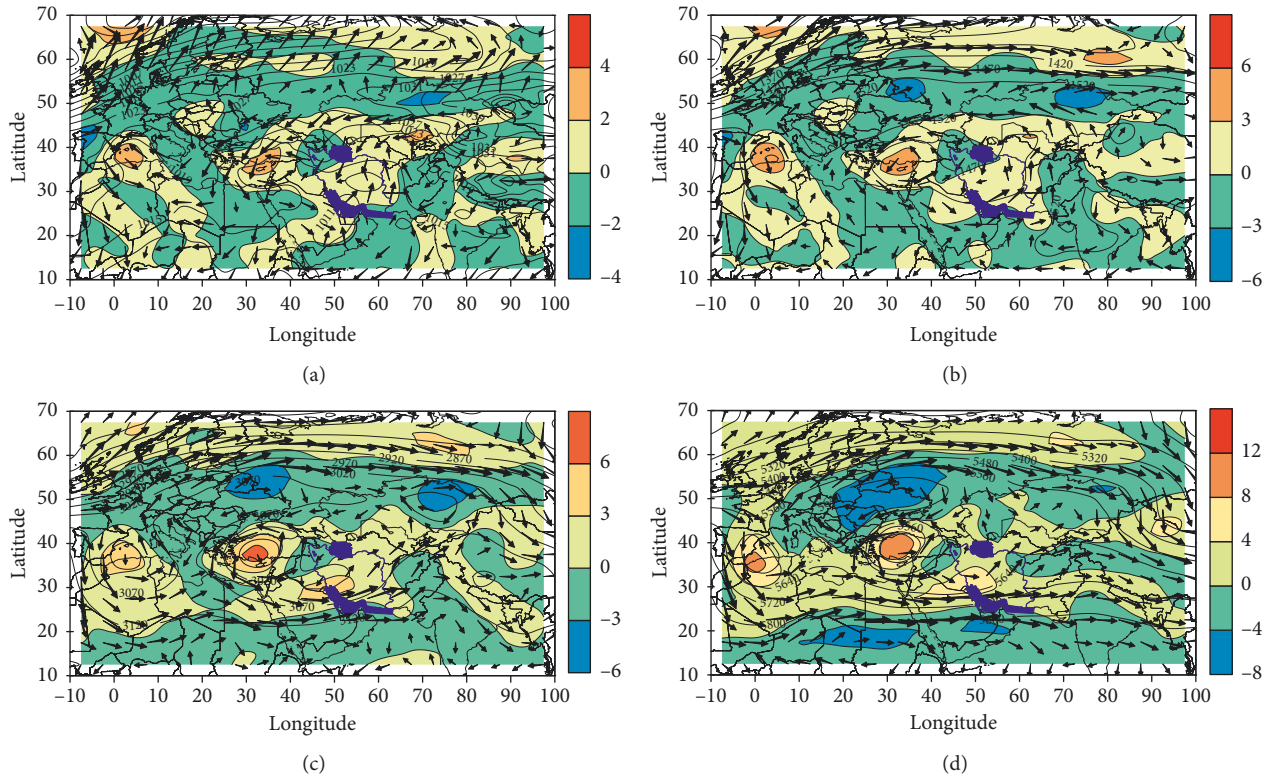

FIGURE 3: (a) 1000 hPa height (contours), vorticity ($5 \times 10^{-5}_{S^{-1}}$) (shaded), and wind flow (m/s) (vectors). (b) 850 hPa height, vorticity ($5 \times 10^{-5}_{S^{-1}}$), and wind flow (m/s). (c) 700 hPa height, vorticity ($5 \times 10^{-5}_{S^{-1}}$), and wind flow (m/s). (d) 500 hPa height, vorticity ($5 \times 10^{-5}_{S^{-1}}$), and wind flow (m/s).

geopotential meters is placed on the south of Turkey and East Mediterranean. The altitude trough is seen on the southwest and the Persian Gulf as positive vorticity advection on Iran causes a rise in the undercurrent convergence and vertical velocity of the air at the upper levels. At the 500 hPa level in Figure 3(d) on the southwest of the country, the altitude trough with positive vorticity advection of $8 \times 10^{-5}_{S^{-1}}$ shows convergence of rising flows of lower levels and upper level divergence. As a result of these conditions, the ground low pressure is constantly strengthened and deepened especially if it is accompanied with adequate moisture. After forming along the southwestern-northeast, the flows of the trough move to higher latitudes [48] and are converted to a dynamic mode and cause prevalent precipitation on Iran. In this pattern, the cyclone located on Iran is a dynamic system that synchronizes with the synoptic system of the middle levels of the atmosphere. This synoptic arrangement on Iran, with the supply of moisture from the Mediterranean and the Persian Gulf, has had a particular dynamic situation in the incidence of prevalent precipitation.

3.2. The Second Pattern: Central Iran Closed Low Pressure-High Pressure of Europe. In this model, according to Figure 4(a) on a map of 1000 hPa level, a low-pressure area with centrality of 1010 hPa and 1000 hPa as an inverse pressure trough is completely placed on the central plateau of Iran. The stretch of the south flows towards the low-pressure north on Iran and causes the reduction of airflow and airflow divergence on Iran and negative vorticity advection of $-3 \times 10^{-5}_{S^{-1}}$. On the other hand, on Central Europe, the high-pressure trough of 1022 hPa passes over the Black Sea and the Mediterranean and moves towards the lower latitudes in the central region of the Red Sea. This pressure arrangement is associated with the transmission of high-latitude cold and wet weather. In the upper level of 850 hPa (Figure 4(b)), we see low-height center of the Urals that is placed at a high level and west of the low-pressure center of land surface.

Moving up from the ground level, the low-height center of the upper level tends to move toward the northwest. In this level, convergence of degradation flows is observed behind the low-height trough where the negative vorticity advection of $-3 \times 10^{-5}_{S^{-1}}$ is placed to the north of the Red Sea and East Mediterranean. In contrast, the southern and eastern half of the country is placed on the elevation range of the trough and positive vorticity advection on the axis of the trough derived from the Urals low-height center on the west and southwest of $3 \times 10^{-5}_{S^{-1}}$,causing the highest amount of convergence at 850 hPa. On the other hand, studying the maps of the higher levels of 700 and 500 hPa shows that, similar to 850 hPa of height, a trough with centrality of 2980 geopotential meter is placed on the border to the west of the country and the Persian Gulf (Figures 4(c) and 4(d)). Positive vorticity advection of $5 \times 10^{-5}_{S^{-1}}$ per second coincides

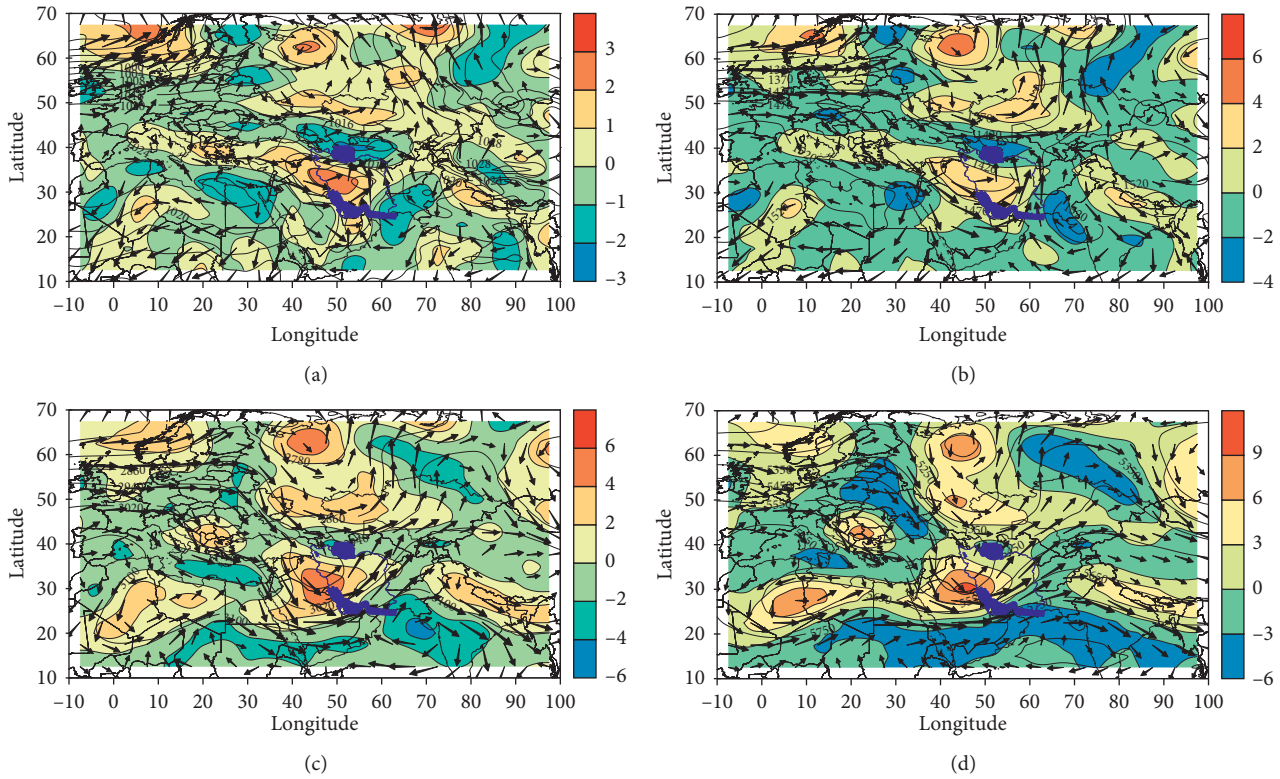

Figure 4: (a) 1000 hPa height (contours), vorticity ($5 \times 10^{-5}_{S^{-1}}$) (shaded), and wind flow (m/s) (vectors). (b) 850 hPa height, vorticity ($5 \times 10^{-5}_{S^{-1}}$), and wind flow (m/s). (c) 700 hPa height, vorticity ($5 \times 10^{-5}_{S^{-1}}$), and wind flow (m/s). (d) 500 hPa height, vorticity ($5 \times 10^{-5}_{S^{-1}}$), and wind flow (m/s).

with the axis of the trough. The convergence of subsurface flows and maximum upside cyclonic movements in 700 hPa all over of Iran were observed at 500 hPa level as its two lower levels. The axis of low height trough with centrality 5440 geopotential meter and positive vorticity advection with amount of $7 \times 10^{-5}_{S^{-1}}$ coincide with the low height axis is placed on Iraq and Saudi Arabia. Convergence and descending of northern cold flows in the western slope are clearly observed. It is observed that, in the higher layers of the atmosphere, just above the surface low-pressure center on Iran, the weather is divergent and air climbing from the lower layer is extended and exits from the rising air. The low-height center of the levels of 850, 700, and 500 hPa are placed under the area of upper level divergence. As a result, the deep divergence in the upper layers caused the forced air vertically in lower layers. As a result, low-pressure system of ground is strengthened and positive vorticity advection and convergence of airflow occur in lower levels and continue up to 500 hPa in Iran in lower levels and continues up to 500 hPa on Iran. In this pattern, there was a short wave at the middle level, and positive vorticity at the lower level of the atmosphere. These dynamic systems have provided ascending conditions. Eventually, with the provision of moisture by the Oman Sea and the Persian Gulf, the dynamic system has caused prevalent precipitation in Iran.

3.3. The Third Pattern: Low Pressure of the Urals-High Pressure of the Middle East. According to Figure 5(a), at the 1000 hPa level, a very strong low-pressure center of 990 hPa with several closed curves is placed on the west of Russia widely. Two pressure tongues are derived from it; one is with pressure of 1010 hPa in a southwesterly direction drawn through the Black Sea to the Mediterranean. The other tongue is in the southeast, crossing the Caspian to central areas of Iran (1014 hPa). This situation has led to taking sufficient moisture by passing through the Caspian Sea and transferring it to the central regions of Iran. As a result of such action, widespread precipitation has occurred especially in areas to the southeast of the country. In addition, on the northeast of Africa, Egypt, Syria, Iraq, and Saudi Arabia, a wide area of relatively high pressure of 1022 hPa is observed that in accordance with the low-pressure tongue of the Urals causes positive vorticity advection of $2 \times 10^{-5}_{S^{-1}}$ on the west and northwest of Iran.

At the level of 850 hPa in Figure 5(b), which matches the pressure pattern of 1000 hPa, the Ural low-pressure center is placed on west of Russia with centrality of 1200 geopotential meter. An elevation trough is observed in East Europe and the Mediterranean and on Iran passing from the Caspian Sea to the Persian Gulf. The cold weather of Scandinavia and

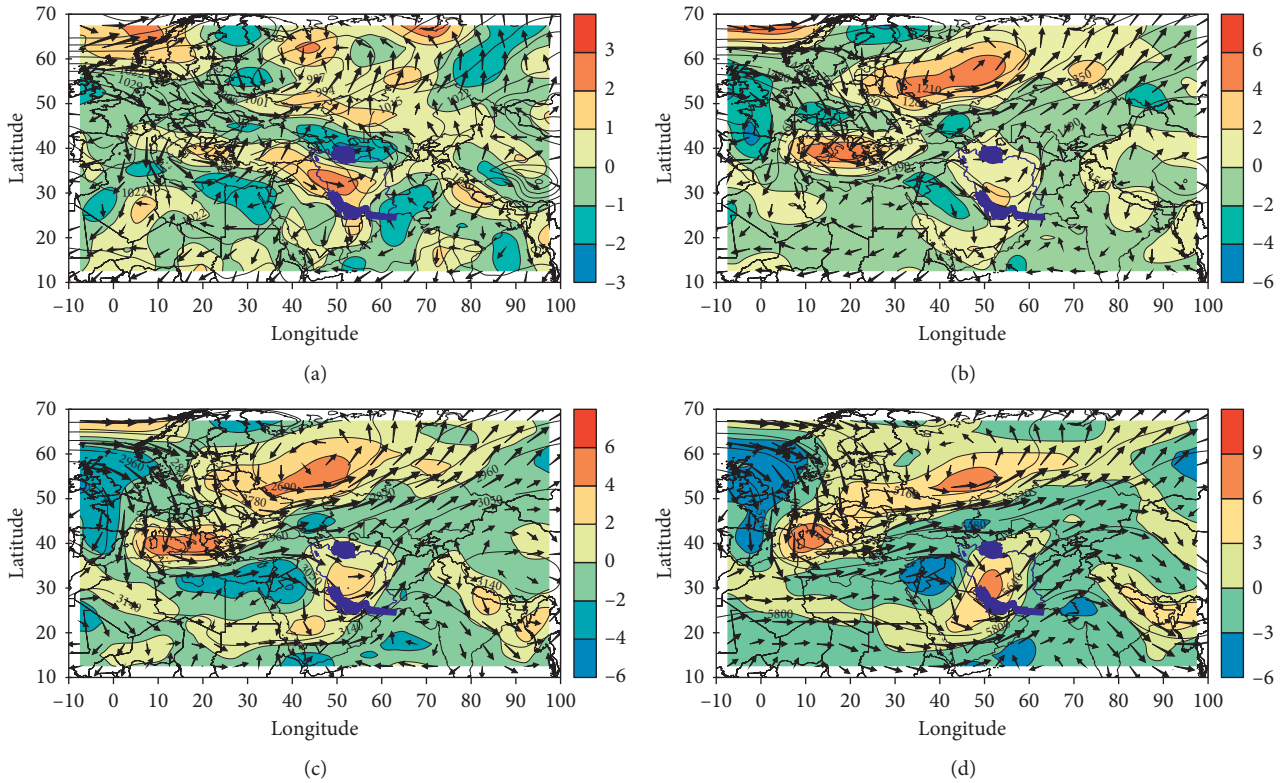

Figure 5: (a) 1000 hPa height (contours), vorticity ($5 \times 10^{-5}_{S^{-1}}$) (shaded), and wind flow (m/s) (vectors). (b) 850 hPa height, vorticity ($5 \times 10^{-5}_{S^{-1}}$), and wind flow (m/s). (c) 700 hPa height (hPa), vorticity ($5 \times 10^{-5}_{S^{-1}}$), and wind flow (m/s). (d) 500 hPa height, vorticity ($5 \times 10^{-5}_{S^{-1}}$), and wind flow (m/s).

Siberia transfers to lower latitudes by the low height centrality and its convergence with wet flows of Mediterranean and the Black Sea from the trough of the Mediterranean and its transfer to Iran by a relatively deep trough, based on the center of the country. In its movement from stack to the trough, the air has downward movement and with convergence, so the trough is the center of positive vorticity advection with amount of $2 \times 10^{-5}_{S^{-1}}$ and the maximum of convergence located on the trough axis [5, 47]. At the levels of 700 and 500 hPa, Figures 5(c) and 5(d), an elevation model of 850 hPa can also be clearly observed. Negative vorticity advection of $-4.5 \times 10^{-5}_{S^{-1}}$ is placed on East Mediterranean and the east of Iraq and Jordan. It causes reduction and air convergence at the trough axis and rising flows in front of the trough at this level. On the other hand, vorticity advection at the 700 hPa level of $3 \times 10^{-5}_{S^{-1}}$ on the trough axis is centered on Iran and its eastern slope of elevation. Convergence of cyclonic flows and rising air masses in these areas, especially the eastern half of the country, can be observed. As it can be observed, on the upper level (i.e., 500 hPa), the trough axis based on Iran is drawn with slight change to the below layers on the southwest areas of the Persian Gulf and lower latitudes to Saudi Arabia. The deepening trough above leads to durable stability and convergence of the flows related to Mediterranean, northern parts of the Red Sea, the Persian Gulf, and the Sea of Oman. As in front of the trough (its east range), positive vorticity advection of $6 \times 10^{-5}_{S^{-1}}$ leads to the severe divergence of uppermost level, convergence of undercurrent, and thus, the formation of heavy precipitation, especially on the eastern half and south of the country. In fact, the areas are placed in front of the warm front. This convergence in the upper layers leads to the accumulation of air, which is dropped over the high-pressure of its bottom surface. The weather descended is replaced by diverged air at ground level, and even if the thickness of the layer of convergence at higher levels on the thickness of the low-level divergence is more, or in other words, the trough level is closer to the Earth's surface, the high pressure of Middle East is amplified. As a result, this pressure arrangement at different atmospheric levels strengthens the pressure trough on Iran and expands the front part of trough and maximum wind vorticity at the levels of 850, 700, and 500 hPa, and the upper-level divergence on the eastern half of Iran and required dynamic conditions for prevalent precipitation on Iran. In this pattern, a relatively deep trough in the middle level of the atmosphere has been formed on Iran. The establishment of the above situation created and strengthened the Ural low pressure and the high pressure of the east and west of Iran and subsequently made the northern-southern flows intense at the surface and the lower levels of the atmosphere. Therefore, the above two systems flew the cold and moist air from the Caspian Sea, Black Sea, and Mediterranean Sea to Iran. When this cold air crosses the warmer seas, it causes prevalent precipitation in Iran.

3.4. The Fourth Pattern: Low-Pressure of Saudi Arabia and High-Pressure Europe. According to Figure 6(a), at the level of 1000 hPa, a very broad area of high pressure 1030 hPa can be seen on Europe from parts of Scandinavia to the Mediterranean in the south and the east of the borders of Russia. The high-pressure tongue enters the country from the northwest and the Caspian Sea. The establishment of this high-pressure center dramatically increases the circulation in the lower levels of the atmosphere over the entire Caspian Sea region. As it moves into northern parts of the Caspian Sea, the cyclonic circulation increases, and the maximum negative vorticity is observed at the northern end of the Caspian Sea. On the other hand, a broad low-pressure center of 1010 hPa is entirely placed on Saudi Arabia, Iraq, and the Persian Gulf. The high pressure of Europe has created a strong gradient on the Black Sea, Turkey, Iraq, and especially the northern half of the country, and positive vorticity advection of $2.5 \times 10^{-5}_{S^{-1}}$ winds on the country's northwest. The pressure arrangement leads to warm air advection of lower latitudes in the northern half of the country and diffusion of very cold weather in northern Europe to the region. At the 850 hPa level in Figure 6(b), the high height center of 1580 geopotential meters is located perfectly on Europe and its tongue of 1520 geopotential meters on the northern strip. On the other hand, low height center with the amount of 1400 geopotential meters is placed on the north of Kazakhstan with its troughs from the northeast influencing the borders of the country. This height situation led to a convergence of very cold flows of northern Europe and Siberia and its precipitation on the northern regions of the country. On the other hand, the very strong height trough with several contours at 1440 geopotential meters is placed on Iraq and Saudi Arabia. The situation follows the advection of warm and moist currents from the Mediterranean and the Red seas to the Persian Gulf on Iran. Hence, that vorticity advection in the eastern tongue of a low height of $3 \times 10^{-5}_{S^{-1}}$ corresponding to intense flows of north leads to increase of mass and density and increasing convergence pressure in the level above the country.

At the 850 hPa level, the high height of 1580 geopotential meters (Figure 6(b)) is entirely located on Europe, and a tongue of it drawn on the northern strip of Iran (1520 geopotential meters). The deployment of this high pressure leads to a widespread and continuous north-northeast flow in the lower levels on the northern half of Iran. On the other hand, a low-height center of 1,400 geopotential meters is located in northern Kazakhstan, with its tongue infiltrating from the northeast of the borders of Iran. This height features led to the convergence of the very cold currents of northern Europe and Siberia and its downfall over the northern regions of Iran. Besides, a very strong trough is located in Iraq and Saudi Arabia and this situation has led to the convergence of hot and humid currents from the Mediterranean Sea, Red Sea, and Persian Gulf on Iran ($3 \times 10^{-5}_{S^{-1}}$). In these conditions, the vorticity convergence of the eastern tongue of low height has been adapted to the northward currents on Iran. As a result, all of these situations lead to increase in mass and density of airflow on the country, which has resulted in an increase in pressure and convergence at the 850 hPa level.

At the 700 hPa level in Figure 6(c), the height arrangement of the lower level is affected by the south elevation trough, whose center of 3000 geopotential meters is placed on southern Turkey, Iraq, Syria, and East Mediterranean. Transfer of moisture from the Mediterranean Sea, the Red Sea, and the Persian Gulf, especially positive vorticity advection of $2.5 \times 10^{-5}_{S^{-1}}$, can be observed on the eastern slopes of the trough. At the 500 hPa level in Figure 6(d), the lower level of the axis of the southern trough, perfectly on the Red Sea and the middle of it, is drawn. The positive vorticity advection area corresponding to the trough with amount of $7 \times 10^{S^{-1}}_{-5}$ intensifies the divergence in upper levels and convergence in the lower levels. Saudi Arabia has low-pressure condition, and there are enhanced uplink moves in Iran and the Middle East by intensity of divergence in higher levels. Due to the establishment of a relatively deep trough at the midlevels between the Caspian Sea and the Aral Lake, the vorticity on the northern regions, especially the eastern parts of the Caspian Sea, are mostly positive, and in the surface map, a low pressure or cyclonic circulation dominated on the Aral Lake. In contrast, at the surface, a dynamic high pressure has been established on the whole region of the southern part of the Caspian Sea and the regions between the Caspian Sea and the Black Sea [49]. These conditions and the location of the low pressure of Saudi Arabia on the southern half of Iran have led to a fairly severe vorticity convergence at the lower and middle levels of the Iran's atmosphere. These features provided the climbing conditions, especially in the northern half of the country, and have caused the widespread precipitation in Iran.

In the precipitation pattern, with the outbreak of widespread precipitation on Iran leading to the release of latent heat of vaporization of rain, it added to the intensity of flotation and uplink movements. By intensifying uplink movements and expansion of air, the vorticity of the system is further increased, and by intensifying the vorticity of low height centers on the Middle East, it added to the severity of divergence in the upper levels of the atmosphere. In this pattern, at the middle level of the atmosphere, the front part of the trough with direction of northeast-southwest is located on Iran. The southward expansion of this trough has strengthened the surface low pressure. Therefore, with the availability of ascending conditions and with the humidity advection from the Mediterranean Sea and the Persian Gulf water resources caused the prevalent precipitation of Iran.

3.5. The Fifth Pattern: High Pressure Belt of Siberia-Central Iran Low Pressure. According to Figure 7(a), the low pressure of central Iran with pressure of the central core of 1010 hPa is placed in Iran in the northeast direction, whose south tongue with north side caused the rising of wet flows from the Sea of Oman and the Persian Gulf on Iran. Negative vorticity advection on Iran of $-1.5 \times 10^{-5}_{S^{-1}}$ can be seen due to the placement of the western part of low pressure on the country and reducing input airflow from north and

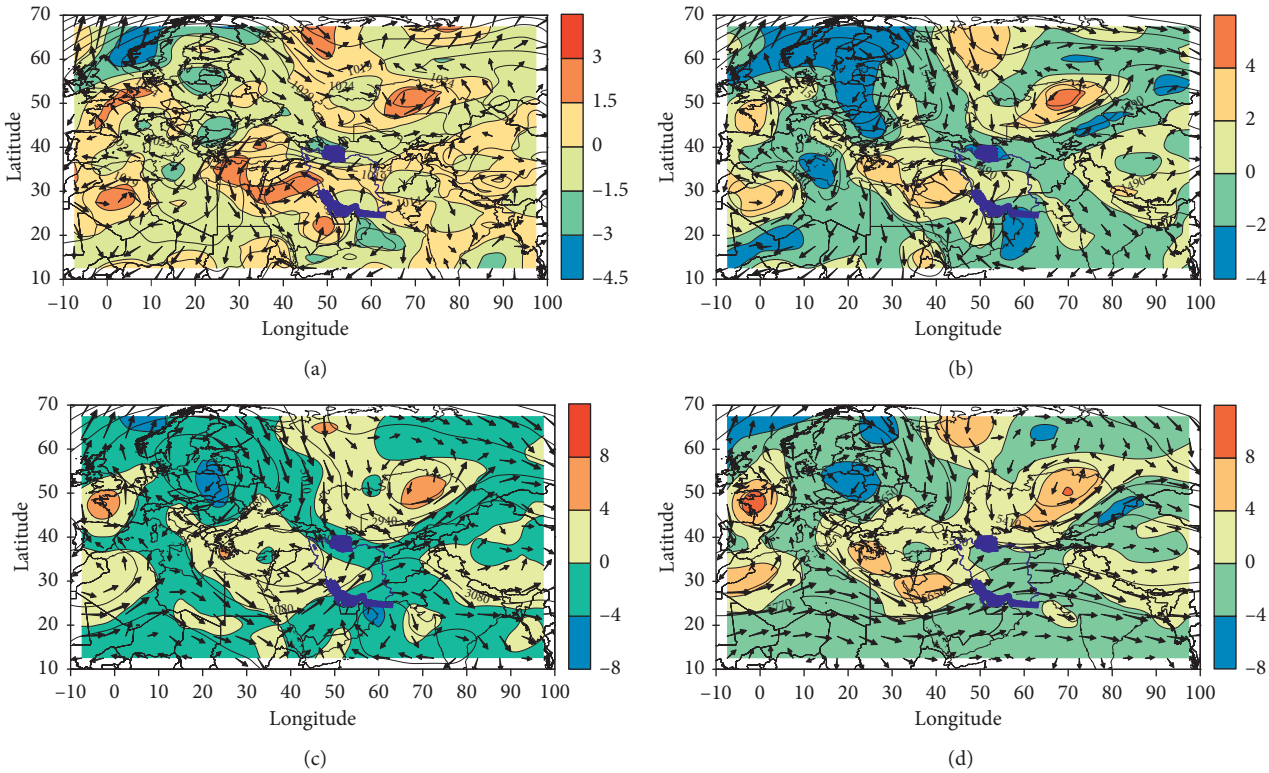

Figure 6: (a) 1000 hPa height (contours), vorticity ($5 \times 10^{-5}_{S^{-1}}$) (shaded), and wind flow (m/s) (vectors). (b) 850 hPa height, vorticity ($5 \times 10^{-5}_{S^{-1}}$), and wind flow (m/s). (c) 700 hPa height, vorticity ($5 \times 10^{-5}_{S^{-1}}$), and wind flow (m/s). (d) 500 hPa height, vorticity ($5 \times 10^{-5}_{S^{-1}}$), and wind flow (m/s).

increasing output mass in the south part of low pressure, reducing mass and the density of pressure, leading to divergence. On the other hand, the Siberian high pressure is reinforced and its range expanded to the northern half of the country causing the loss of cold air, decreasing airflow into the country, and exacerbating the divergence on the surface of the ground. Pressure arrangement of two low-pressure centers in the Persian Gulf and Siberian high pressure caused a sharp pressure and exacerbating instability on the northeastern areas of the country. At 850 hPa in Figure 7(b) as well as sea level, the low-height belt of central Iran with a central height of 1360 and 1400 geopotential meters is placed on Iran and the northeast. Positive vorticity advection on Iran of $3 \times 10^{-5}_{S^{-1}}$, matching the central core of low height, can be seen on Iran. However, this value in northwest reaches $2 \times 10^{-5}_{S^{-1}}$. On the map, at the pressure of 700 and 500 hPa in Figures 7(c) and 7(d), the axis of the trough is placed in the East and Southeast of Iran, and vorticity advection with the amount of $5 \times 10^{-5}_{S^{-1}}$ can be seen in this area. Considering that the placing of low pressure of central Iran in below levels caused the rise and convergence at lower levels of the atmosphere on the eastern and southeastern part and on the northwest of Iran at 700 hPa level, a low height center with center based at 2960 geopotential meters causes rising and convergence in the lower layers of the atmosphere. Positive vorticity advection resonance indicates rising and positive convergence at the levels of 700 and 500 hPa. In this pattern, in the higher layers, air density is reduced, and reducing density increases vertical airflow in the lower layers of the atmosphere. In such a case, the flow of cold weather cools down due to adiabatic flow and causes the column of airflow on low pressure of central Iran to be colder than the surrounding environment, and the thickness of the column of airflow is reduced. Therefore, due to the decrease in the density of the air column at the levels of 850 and 700 hPa, curves at lower altitude are placed at surrounding area and can be seen on maps of 850, 700, and 500 hPa as low height cores (Figures 7(b)–7(d)). According to the process of turning at low pressure on the surface of the Earth (counterclockwise rotation), the flow of cold air is placed behind the low pressure [48, 50]. In other words, the western half of the low pressure of central Iran is colder than the eastern half, so the low-pressure of central Iran is stronger and axis of low pressure with increasing height at the levels of 850, 700, and 500 hPa inclined to the colder weather in the west, and the low-pressure system on Iran extended to southeast-northwest. This pressure arrangement at different atmospheric levels and placement of trough axis on Iran causes the intensity of vorticity advection and vertical rising of air at levels of 1000, 850, 700, and 500 hPa and divergence of air in the upper levels of the atmosphere. In this pattern, the trough axis positioning on the southern half of the country and low pressure on the surface has strengthened the upstream flow and exacerbated the instability in the region. These dynamic conditions have resulted in humidity advection from the Persian Gulf and

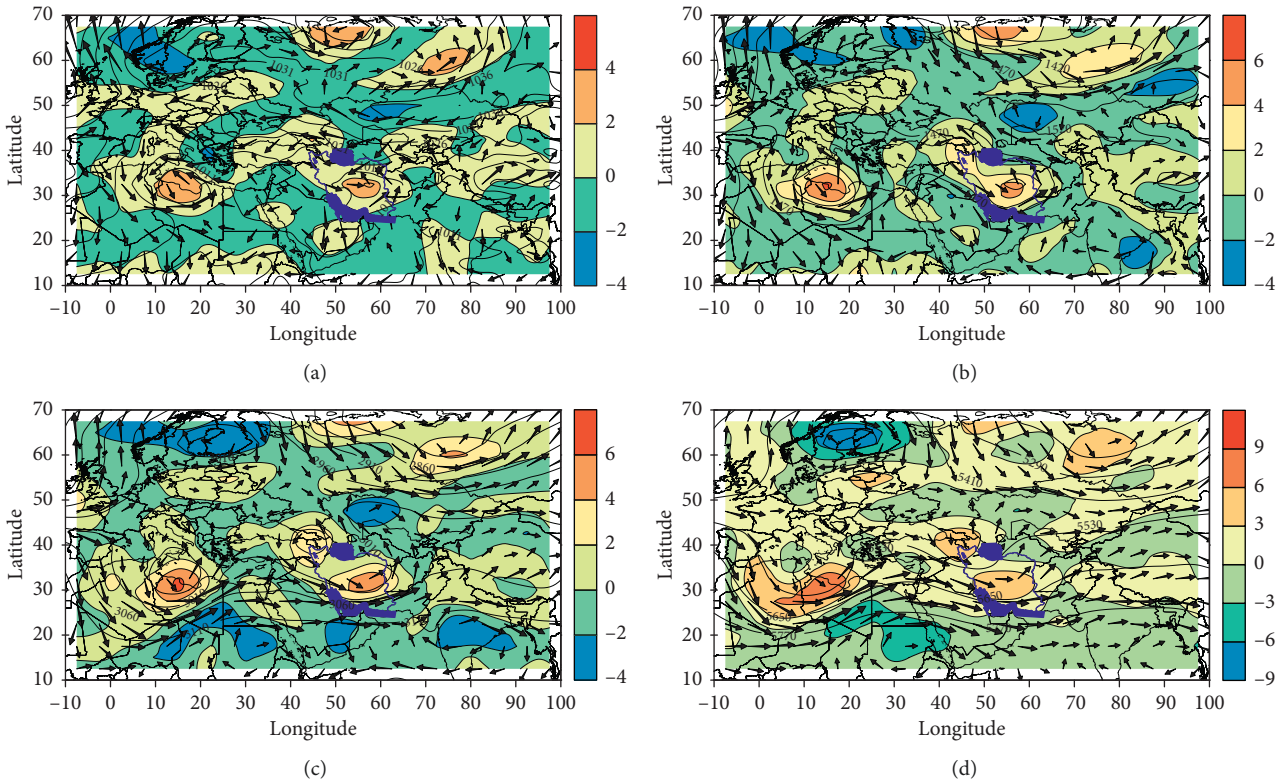

Figure 7: (a) 1000 hPa height (contours), vorticity ($5 \times 10^{-5}_{S^{-1}}$) (shaded), and wind flow (m/s) (vectors). (b) 850 hPa height, vorticity ($5 \times 10^{-5}_{S^{-1}}$), and wind flow (m/s). (c) 700 hPa height, vorticity ($5 \times 10^{-5}_{S^{-1}}$), and wind flow (m/s). (d) 500 hPa height, vorticity ($5 \times 10^{-5}_{S^{-1}}$), and wind flow (m/s).

the Oman Sea to Iran and the formation of prevalent precipitation.

Low-pressure systems have played a major role in the occurrence of winter-prevalent precipitation in Iran in all patterns. By creating instability in the atmosphere, these systems have led to the formation of baroclinic states, especially in the lower level of atmosphere. In the common mechanism of the occurrence of prevalent precipitation in all patterns was the role of midlatitude's trough (such as the Mediterranean trough) in strengthening low-pressure systems of lower levels of atmosphere, as well as the water resources such as the Persian Gulf, the Oman Sea, the Mediterranean Sea, the Caspian Sea, and the Black Sea in the provision of required humidity for that dynamic systems.

4. Conclusion

In this study, the status of vorticity of the atmosphere of pressure centers on Iran and the mechanisms of climate changes on widespread winter precipitation in Iran were investigated. For this purpose, the data of prevalent winter precipitation in Iran were identified on the basis of a millimeter precipitation threshold. After extracting prevalent winter precipitation in Iran, the U&V wind component and pressure data corresponding to the widespread rainy days were extracted from the databases of NCEP/NCAR and vorticities of these days were calculated. Then, by the implementation of cluster analysis, representative days for each group were specified. The results of this study showed that the atmospheric vorticity status during prevalent winter precipitation in Iran is influenced by the interaction of low-pressure patterns of the Persian Gulf double core-low pressure of the East Mediterranean, central Iran closed low pressure-high pressure of Europe, low pressure of the Urals-high-pressure of the Middle East, low pressure of the Urals-high-pressure of Europe, and the high-pressure belt of Siberia-low pressure of central Iran.

In addition, the placement of the low pressure of dual-core of the Persian Gulf-East Mediterranean low pressure on Iran at levels of 850, 700, and 500 hPa of maximum positive vorticity caused rising and convergence of airflow at higher levels and the bottom surfaces. As a result of such conditions, the low pressure of land surface with moisture injected from the Persian Gulf and the Oman Sea and trough on Iran in high levels have strengthened its atmosphere. Positive vorticity advection on Iran is continued up to 500 hPa. In this regard, Alijani et al. investigated Iran's low-pressure role in the intensification of positive vorticity. The results of this study showed that this low pressure was the main cause of moisture transmission and the occurrence of precipitation in the first decade of July 1994 in the southeast of Iran [51]. The formation of this low pressure on the northern side of the Persian Gulf, while increasing the cyclonic motion in the southern part of the country, by creating suitable southern streams in the southeast of Iran and transferring the moisture content of the Oman Sea in a thin layer to the

studied area caused the extreme precipitation in southeastern Iran.

However, at the time of central Iran closed low pressure-high pressure of Europe, the center of low pressure on Iran caused convergence and rising airflow to higher latitudes. The placement of trough axis at levels of 850, 700, and 500 hPa caused increased positive vorticity advection on Iran and rising air in the lower atmosphere layers and divergence in the upper levels of the atmosphere. Therefore, the positive vorticity maximum is continued up to 500 hPa. In fact, the high pressure on the Middle East and the influence of the low-pressure tongue of the Urals on Iran and closing of the surface of trough to the Earth's surface caused the high pressure of Middle East to strengthen.

As a result of this pressure arrangement at different levels of the atmosphere, the pressure trough on Iran is strengthened. These conditions exacerbated dynamic conditions for the occurrence of widespread precipitation on Iran. On the other hand, the influence of the low-pressure tongue in Saudi Arabia on Iran at the ground level caused positive vorticity advection and influenced north flowing towards Iran. The low pressure of Saudi on Earth strengthened itself by the exposure to the wave of west wind at higher levels and exacerbated the divergence, leading to strengthened rising movements on Iran. Latent heat of vaporization of precipitation led to strengthening the uplink flow on Iran with these conditions increasing by strengthening the uplink flows and expansion and vorticity of the system, causing divergence in the upper levels of atmosphere. Vorticity state of the atmosphere during the formation of the central Iran low pressure made the flow of cold weather in the western half of low pressure placed on Iran colder than its eastern half. This strengthens the central Iran low pressure and causes the inclination of the low-pressure axis at levels of 850, 700, and 500 hPa in the western and northwestern areas in Iran. Pressure arrangement in different atmospheric levels and placing trough axis on Iran led to intensifying the positive vorticity advection on Iran. In the studies of Golmohammadian and Pishvaei about the production of daily rotation index and its effect on the temperature and precipitation of the northeastern part of Iran, it has been concluded that during the warm seasons, a ridge pattern has an absolute sovereignty in this region, which represents the emergence of a tropical belt on the area. As a result, Mashhad has a warm and dry climate in the warm seasons, while this cannot be seen in the cold seasons [52]. The average monthly vorticity indicator in the coldest half of the year has the highest value, indicating the frequency of cyclonic systems. In most cases, increasing the vorticity rate in one region leads to a decrease in temperature and an increase in precipitation. The major difference between the third and fourth patterns with other patterns is that the low-pressure systems of these patterns have an origin from the outside of the Iran. But in the first, second, and fifth patterns, the core of the low-pressure systems has been formed inside Iran.

Conflicts of Interest

The authors declare that they have no conflicts of interest.

Acknowledgments

This work was supported by Vedurfelagid, Rannis, and Rannsoknastofa I Vedurfraedi. Iman Rousta is deeply grateful to his supervisor (Haraldur Olafsson, Professor of Atmospheric Sciences, Department of Physics, University of Iceland, Institute for Atmospheric Sciences and Icelandic Meteorological Office), for his great support, kind guidance, and encouragement.

References

[1] I. Rousta, M. Nasserzadeh, M. Jalali et al., "Decadal spatial-temporal variations in the spatial pattern of anomalies of extreme precipitation thresholds (case study: northwest Iran)," *Atmosphere*, vol. 8, no. 12, p. 135, 2017.

[2] C. Data, *Guidelines on Analysis of Extremes in a Changing Climate in Support of Informed Decisions for Adaptation*, World Meteorological Organization, Geneva, Switzerland, 2009.

[3] A. Taimor, A. Qhasem, and I. Rousta, "Analyzing of 500 hpa atmospheric patterns in the incidence of pervasive and sectional rainfall in Iran," *Planning and arrangement of space*, vol. 16, no. 4, pp. 1–24, 2012.

[4] M. Soltani, I. Rousta, and S. S. M. Taheri, "Using Mann–Kendall and time series techniques for statistical analysis of long-term precipitation in gorgan weather station," *World Applied Sciences Journal*, vol. 28, no. 7, pp. 902–908, 2013.

[5] I. Rousta, M. Doostkamian, E. Haghighi, H. R. G. Malamiri, and P. Yarahmadi, "Analysis of spatial autocorrelation patterns of heavy and super-heavy rainfall in Iran," *Advances in Atmospheric Sciences*, vol. 34, no. 9, pp. 1069–1081, 2017.

[6] I. Rousta, M. Soltani, W. Zhou, and H. H. N. Cheung, "Analysis of extreme precipitation events over central plateau of Iran," *American Journal of Climate Change*, vol. 5, no. 3, p. 297, 2016.

[7] M. Soltani, P. Laux, H. Kunstmann et al., "Assessment of climate variations in temperature and precipitation extreme events over Iran," *Theoretical and Applied Climatology*, vol. 126, no. 3, pp. 775–795, 2016.

[8] I. Rousta, M. Doostkamian, A. Taherian, E. Haghighi, H. G. Malamiri, and H. Ólafsson, "Investigation of the spatio-temporal variations in atmosphere thickness pattern of Iran and the middle east with special focus on precipitation in Iran," *Climate*, vol. 5, no. 4, p. 82, 2017.

[9] I. Rousta, M. Doostkamian, E. Haghighi, and B. Mirzakhani, "Statistical-synoptic analysis of the atmosphere thickness pattern of Iran's pervasive frosts," *Climate*, vol. 4, no. 3, p. 41, 2016.

[10] J. R. Harman, *Synoptic Climatology of the Westerlies: Process and Patterns*, Association of American Geographers, Washington, DC, USA, 1991.

[11] L. A. Mofor and C. Lu, "Generalized moist potential vorticity and its application in the analysis of atmospheric flows," *Progress in Natural Science*, vol. 19, no. 3, pp. 285–289, 2009.

[12] N. R. Council, *The Atmospheric Sciences: Entering the Twenty-First Century*, The National Academies Press, Washington, DC, USA, 1998.

[13] M. Soltani, P. Zawar-Reza, F. Khoshakhlagh, and I. Rousta, "Mid-latitude cyclones climatology over Caspian Sea Southern Coasts–North of Iran," in *Proceedings of 21st Conference on Applied Climatology*, pp. 1–7, American Meteorological Society (AMS), London, UK, 2014, https://ams.

confex.com/ams/21Applied17SMOI/webprogram/Paper246601.html.

[14] T. Dessouky and A. Jenkinson, "An objective daily catalogue of surface pressure, flow, and vorticity indices for Egypt and it's use in monthly rainfall forecasting," *Meteorological Research Bulleting, Egypt*, vol. 11, pp. 1–25, 1975.

[15] A. Jenkinson and F. Collison, "An initial climatology of gales over the North Sea," *Synoptic Climatology Branch Memorandum*, vol. 62, p. 18, 1977.

[16] D. Conway and P. Jones, "The use of weather types and air flow indices for GCM downscaling," *Journal of Hydrology*, vol. 212, pp. 348–361, 1998.

[17] P. Jones, M. Hulme, and K. Briffa, "A comparison of Lamb circulation types with an objective classification scheme," *International Journal of Climatology*, vol. 13, no. 6, pp. 655–663, 1993.

[18] R. M. Trigo and C. C. DaCAMARA, "Circulation weather types and their influence on the precipitation regime in Portugal," *International Journal of Climatology*, vol. 20, no. 13, pp. 1559–1581, 2000.

[19] I. Phillips and G. McGregor, "The relationship between synoptic scale airflow direction and daily rainfall: a methodology applied to Devon and Cornwall, South West England," *Theoretical and Applied Climatology*, vol. 69, no. 3, pp. 179–198, 2001.

[20] H. Nakamura, "Horizontal divergence associated with zonally isolated jet streams," *Journal of the atmospheric sciences*, vol. 50, no. 14, pp. 2310–2313, 1993.

[21] M. R. Sinclair, "A diagnostic study of the extratropical precipitation resulting from Tropical Cyclone Bola," *Monthly Weather Review*, vol. 121, no. 10, pp. 2690–2707, 1993.

[22] C. Mattocks and R. Bleck, "Jet streak dynamics and geostrophic adjustment processes during the initial stages of lee cyclogenesis," *Monthly Weather Review*, vol. 114, no. 11, pp. 2033–2056, 1986.

[23] R. A. Maddox and C. A. Doswell, "An examination of jet stream configurations, 500 mb vorticity advection and low-level thermal advection patterns during extended periods of intense convection," *Monthly Weather Review*, vol. 110, no. 3, pp. 184–197, 1982.

[24] D. G. Vincent, "Cyclone development in the south pacific convergence zone during fgge, 10-17 January 1979," *Quarterly Journal of the Royal Meteorological Society*, vol. 111, no. 467, pp. 155–172, 1985.

[25] G. Wang, J. Su, Y. Ding, and D. Chen, "Tropical cyclone genesis over the South China Sea," *Journal of Marine Systems*, vol. 68, no. 3, pp. 318–326, 2007.

[26] P. Alpert, B. Neeman, and Y. Shay-El, "Climatological analysis of Mediterranean cyclones using ECMWF data," *Tellus A: Dynamic Meteorology and Oceanography*, vol. 42, no. 1, pp. 65–77, 1990.

[27] A. Bartzokas and D. Metaxas, *Climatic Fluctuation of Temperature and Air Circulation in the Mediterranean*, Commission of the European Communities (CEC), Europe, 1991.

[28] N. Ruiz and W. Vargas, "500 hPa vorticity analyses over Argentina: their climatology and capacity to distinguish synoptic-scale precipitation," *Theoretical and Applied Climatology*, vol. 60, no. 1–4, pp. 77–92, 1998.

[29] E. Xoplaki, J. F. González-Rouco, J. Luterbacher, and H. Wanner, "Wet season Mediterranean precipitation variability: influence of large-scale dynamics and trends," *Climate dynamics*, vol. 23, no. 1, pp. 63–78, 2004.

[30] G. Hadis and P. Mohammad Reza, "Daily vorticity index and it's impacts on precipitation and temperature in Khorassan region in 1948-2010," *Journal of Applied Researches in Geographical Sciences*, vol. 13, no. 29, pp. 217–236, 2013.

[31] B. Alijani and M. Zahehi, "Statistical and synoptic analysis of Azerbaijan area rainfall," *Iranian Journal of Research in Geography*, pp. 65-66, 2002.

[32] M. Mohammad Hossain and M. Mohammad, "investigating pressure trough of Red Sea from the perspective of the dynamic," *Nivar*, vol. 52, pp. 67–74, 2004.

[33] A. Mofidi, A. Zarrin, and G. R. J. Ghobadi, "Determining the synoptic patterns of autumn-time extreme and severe precipitation over the southern coasts of Caspian Sea," *Journal of the Earth and Space Physics*, vol. 33, no. 3, p. 30, 2008.

[34] E. Kalnay, M. Kanamitsu, R. Kistler et al., "The NCEP/NCAR 40-year reanalysis project," *Bulletin of the American Meteorological Society*, vol. 77, no. 3, pp. 437–471, 1996.

[35] B. E. Doty and J. L. I. Kinter, *Geophysical Data Analysis and Visualization Using the Grid Analysis and Display System*, National Aeronautics and Space Administration, Washington, DC, USA, 1995.

[36] J. E. Martin, *Mid-Latitude Atmospheric Dynamics: a First Course*, John Wiley & Sons, Hoboken, NJ, USA, 2013.

[37] M. R. Kaviani and B. Alijani, *Principles of Climatology*, SAMT Press, Tehran, Iran, 1st edition, 2001.

[38] K. E. Trenberth, "Recent observed interdecadal climate changes in the Northern Hemisphere," *Bulletin of the American Meteorological Society*, vol. 71, no. 7, pp. 988–993, 1990.

[39] B. J. Hoskins and K. I. Hodges, "New perspectives on the Northern Hemisphere winter storm tracks," *Journal of the Atmospheric Sciences*, vol. 59, no. 6, pp. 1041–1061, 2002.

[40] E. K. Chang and D. B. Yu, "Characteristics of wave packets in the upper troposphere. Part I: Northern Hemisphere winter," *Journal of the Atmospheric Sciences*, vol. 56, no. 11, pp. 1708–1728, 1999.

[41] B. Alijani, J. O'Brien, and B. Yarnal, "Spatial analysis of precipitation intensity and concentration in Iran," *Theoretical and Applied Climatology*, vol. 94, no. 1, pp. 107–124, 2008.

[42] H. Lashkari, Z. Mohammadi, and G. Keikhosravi, "Annual fluctuations and displacements of inter tropical convergence zone (ITCZ) within the range of Atlantic Ocean-India," *Open Journal of Ecology*, vol. 7, no. 1, p. 12, 2017.

[43] E. Haghighi, S. Jahanbakhsh, M. R. Banafshe, and I. Rousta, "The study relationship between large-scale circulation patterns of sea level and snow phenomenon in the North West of Iran," *Territory*, vol. 12, no. 48, pp. 19–35, 2016, in Persian.

[44] G. Azizi, H. Mohammadi, M. Karimi Ahmadabad, A. Shamsipour, and I. Rousta, "Identification and analysis of the north atlantic blockings," *International Journal of Current Life Sciences*, vol. 5, no. 4, pp. 577–581, 2015.

[45] G. Azizi, H. Mohammadi, M. Karimi Ahmadabad, A. Shamsipour, and I. Rousta, "The relationship between the Arctic oscillation and North Atlantic blocking frequency," *Open Journal of Atmospheric and Climate Change*, vol. 1, pp. 1–9, 2015.

[46] P. D. Williams, "A proposed modification to the Robert–Asselin time filter," *Monthly Weather Review*, vol. 137, no. 8, pp. 2538–2546, 2009.

[47] Y. G. Rahimi, *Synoptic Analysis with GrADS Software*, vol. 2, SAHA Danesh Press, Tehran-Iran, 1st edition, 2016, in Persian.

[48] G. Keykhosrowi and H. Lashkari, "Analysis of the relationship between the thickness and height of the inversion and the severity of air pollution in Tehran," *Journal of Geography and Planning*, vol. 18, no. 9, pp. 231–257, 2014.

[49] G. R. Janbaz Ghobadi, A. Mofidi, and A. Zarrin, "Identify synoptic patterns of heavy rainfall in the summer on the southern shores of the Caspian Sea," *Geography and Planning*, vol. 22, no. 2, pp. 23–39, 2011.

[50] I. Rousta, F. K. Akhlagh, M. Soltani, and S. S. M. Taheri, "Assessment of blocking effects on rainfall in northwestern Iran," in *Proceedings of COMECAP 2014*, p. 291, Crete University Press, Heraklion, Grecce, 2014.

[51] B. Alijani, A. Mofidi, Z. Jafarpour, and A. Aliakbari-Bidokhti, "Atmospheric circulation patterns of the summertime rainfalls of southeastern Iran during July 1994," *Earth and Space physics*, vol. 37, no. 3, pp. 205–227, 2012.

[52] H. Golmohammadian and M. R. Pishvaei, "Production of daily rotation index and its effect on temperature and precipitation of Khorasan region in the period of 1948-2010," *Journal of Applied researches in Geographical Sciences*, vol. 13, no. 29, pp. 217–236, 2013.